Quasienergy-band structure of a periodically driven system with translational symmetry

Syuji Miyazaki and Andrey R. Kolovsky
Fachbereich Physik, Universität Gesamthochschule Essen,
45117 Essen, Federal Republic of Germany
(Received 16 March 1994)

We discuss the quasienergy-band structure for a periodically driven system with translational symmetry. The parameter is so fixed that a bounded fully developed chaotic region is surrounded by regular orbits. Due to the periodicity both in space and in time, eigenvalues of the Floquet operator (quasienergies) form band structures. Its two distinct dispersion relations make it possible to divide each of the bands into *chaotic* and *regular* parts. Transitions between the two parts occur at the points of avoided crossings. Some regular parts are combined into a regular band with a diabatic transformation from the quasienergy basis to a coupled basis in which the avoided crossings are approximately replaced by real crossings. After the regular bands are removed, the nearest-neighbor-spacing statistics of the remaining bands are fitted by the Brody distribution.

PACS number(s): 05.45.+b, 03.65.−w

I. INTRODUCTION

The statistical description of (quasi)energy levels is one of the most popular and successful approaches in the realm of *quantum chaos* [1–4]. In the present paper, our main interest is quantal manifestation of classical chaos in quasienergy-band structure. We will show some nearest-neighbor-spacing statistics of the quasienergy bands for a system driven by a periodic field with translational symmetry.

When discussing avoided crossings and level statistics in the quasienergy spectrum it is necessary to first separate the symmetry classes of the spectrum. In order to avoid this operation, we consider here a desymmetrized version of the double resonance model studied in Ref. [5]. Namely, we consider the system with the Hamiltonian

$$H(x,p;t) = \frac{p^2}{2} - [\cos\omega t + \tfrac{1}{2}\cos(2\omega t + \beta)] \times [\cos x + \tfrac{1}{2}\cos(2x+1)]. \quad (1)$$

The Hamiltonian has no such symmetry $H(x+\pi, p; t+\pi/\omega) = H(x,p;t)$ nor $H(-x,p;t) = H(x,p;t)$ that the double resonance model has. The phase space of the system (1) consists of the region of the chaotic and regular motion (see Fig. 1), as it is generic for realistic systems like a small junction or a superlattice [6]. In addition, choosing the parameter $\beta \neq 0$, we can also consider the case without T (time-reversal) invariance.

In the quantum-mechanical treatment the properties of the system (1) are completely determined by the quasienergy bands and the time-dependent Bloch functions. Reflecting the two different (chaotic and regular) regions in phase space, the band structure of the system (1) consists of two different dispersion relations, and the Bloch functions show correspondingly two different characteristics. Furthermore, there exist avoided crossings at which the two different dispersion relations are interchanged. The existence of avoided crossings in the present case means a kind of nonadiabatic effect anagolous to multiphoton resonance in quantum optics. Thus each of the bands may be partially regular and partially chaotic depending on Bloch wave number. It is, therefore, impossible to separate the bands into *regular bands* and *chaotic bands* over the whole range of wave number. However, with the help of a transformation such avoided crossings can be approximately replaced by real crossings and the quasienergy bands are reconstructed into either regular or chaotic transformed bands. The regular band can be assigned to a classical regular trajectory satisfying the condition

$$\frac{1}{2\pi}\int_{-\pi}^{\pi} p\,dx = l\hbar \quad (2)$$

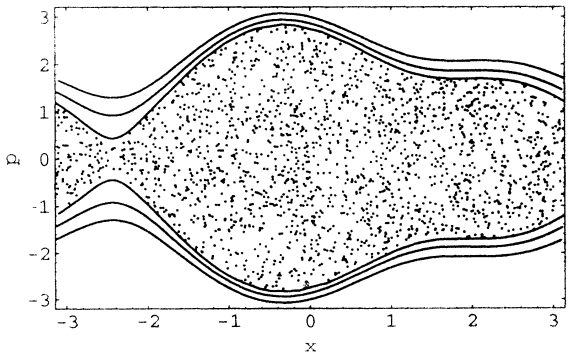

FIG. 1. Poincaré section at $t = n\tau$ ($\tau = 2\pi/\omega$, $n = 1, 2, \ldots$) for $(\omega, \beta) = (0.2, 0)$ in Eq. (1) with T invariance. Chaotic region is created by a single initial point. Regular trajectories satisfying Eq. (2) with $l = \pm 9, \pm 10, \pm 11$ are also shown. The position x is here defined mod 2π.

for an integer l. For a fixed set of parameters $(\omega,\beta) = (0.2,0)$, we can find such trajectories with $|l| \geq 9$ (see Fig. 1). On the other hand, we cannnot find such a correspondence for the chaotic bands, and therefore we need a statistical description.

The quasienergy bands for the system (1) are constructed in Sec. II. We suggest a numerical method of reconstructing the quasienergy bands into regular and chaotic ones with the help of the diabatic transformation in Sec. III. We consider the nearest-neighbor-spacing statistics of the chaotic bands in Sec. IV. The last section is devoted to some concluding remarks.

II. CONSTRUCTION OF QUASIENERGY BANDS

Writing the wave function $\psi(x,t)$ in a generalized Bloch form

$$\psi(x,t) = \frac{1}{\sqrt{2\pi}} \int_{-1/2}^{1/2} dk \varphi^{(k)}(x,t) e^{ikx}, \tag{3a}$$

we obtain the stroboscopic temporal evolution of the Bloch function $\varphi^{(k)}(x,t)$ $[= \varphi^{(k)}(x+2\pi,t)]$ with wave-number-dependent Floquet operator $\hat{F}^{(k)}(t_0)$

$$\varphi^{(k)}(x,t_0+m\tau) = [\hat{F}^{(k)}(t_0)]^m \varphi^{(k)}(x,t_0), \tag{3b}$$

$$\hat{F}^{(k)}(t_0) = \hat{T} \exp\left[-\frac{i}{\hbar}\int_{t_0}^{t_0+\tau} \hat{H}^{(k)}(x,t)dt\right], \tag{3c}$$

$$\hat{H}^{(k)}(x,t) = \frac{\hbar^2}{2}\left(-i\frac{\partial}{\partial x}+k\right)^2 - [\cos\omega t + \tfrac{1}{2}\cos(2\omega t+\beta)] \times [\cos x + \tfrac{1}{2}\cos(2x+1)], \tag{3d}$$

where $m = 1,2,\ldots$, $\tau = 2\pi/\omega$, and $\hat{T}$ denotes the time-ordering operator. We consider the case $t_0 = 0$ hereafter. The dimensionless Planck's constant normalized by material constants is here simply denoted by $\hbar$ [5].

We obtain the Floquet operator $\hat{F}^{(k)}$ by solving the Schrödinger equation $i\hbar\partial\varphi^{(k)}(x,t)/\partial t = \hat{H}^{(k)}(x,t)\varphi^{(k)}(x,t)$ with the Hamiltonian given by Eq. (3d). In the interaction picture

$$\varphi^{(k)}(x,t) = \frac{1}{\sqrt{2\pi}} \sum_n c_n^{(k)}(t) \exp[inx] \exp[-\frac{i}{\hbar}\epsilon_{0n}(k)t], \tag{4}$$

the amplitudes $c_n^{(k)}(t)$ satisfy the following equation:

$$\frac{dc_n^{(k)}}{dt} = c_{n+1}^{(k)} g_n^{(k)} - c_{n-1}^{(k)} g_{n-1}^{(k)*} + c_{n+2}^{(k)} h_n^{(k)} - c_{n-2}^{(k)} h_{n-2}^{(k)*}, \tag{5a}$$

$$g_n^{(k)}(t) = \frac{i}{2\hbar}[\cos\omega t + \frac{1}{2}\cos(2\omega t+\beta)] \times \exp\left[-i\hbar\frac{2n+1+2k}{2}t\right], \tag{5b}$$

$$h_n^{(k)}(t) = \frac{ie^{-i}}{4\hbar}[\cos\omega t + \tfrac{1}{2}\cos(2\omega t+\beta)] \times \exp[-2i\hbar(n+1+k)t], \tag{5c}$$

where g^* denotes the complex conjugate of g and

$$\epsilon_{0n}(k) = \frac{(n+k)^2\hbar^2}{2} \tag{6}$$

is a dispersion law of free motion. We integrate Eq. (5) from $t = 0$ to $t = \tau$ with the initial value $c_n^{(k)}(0) = \delta_{nm}$ using the Adams method [7]. The products $c_n^{(k)}(\tau)\exp[-i\epsilon_{0n}(k)\tau/\hbar]$$(n = 0,\pm1,\pm2,\ldots)$ form the mth column of matrix representation $\mathbf{F}^{(k)}$ of $\hat{F}^{(k)}$ in the free rotor basis. We truncate $\mathbf{F}^{(k)}$ into a finite $L \times L$ matrix. When the chaotic region on the Poincaré section is confined approximately in the range $|p| < p_c$ (see Fig. 1), we set L at about twice as much as $p_c/\hbar$.

By solving the eigenvalue matrix equation $\mathbf{F}^{(k)}\vec{\chi}_l(k) = \exp[-i\tau\epsilon_l(k)/\hbar]\vec{\chi}_l(k)$, the discrete quasienergies $\epsilon_l(k)$ are obtained modulo $\hbar\omega$ for a fixed wave number k. It should be noted that Howland proved that the operator $\mathbf{F}^{(0)}$ has a pure point spectrum [8]. Like energy bands of one-dimensional solids, it can be shown that each quasienergy band $\epsilon_l(k)$ satisfies the symmetry $\epsilon_l(k+1) = \epsilon_l(k)$. The T-invariant case has the additional symmetry $\epsilon_l(-k) = \epsilon_l(k)$. Consequently, we have only to consider the interval $\{I(k) \mid 0 \leq k \leq 1/2\}$ in the T-invariant case and $\{I(k) \mid -1/2 \leq k \leq 1/2\}$ otherwise. The numerical calculation can be practically done at discrete values of wave number $k = k_i$. We divide the interval $I(k)$ into 70 equal intervals in our numerical experiment. The neighboring quasienergies are "connected" in such a way that the absolute value of the scalar product of the corresponding eigenvectors $|\vec{\chi}_l(k_i)\cdot\vec{\chi}_l(k_{i+1})|$ takes the maximal value (nearly equal to unity). Thus we obtain a quasienergy band $\epsilon_l(k)$ as a piecewise continuous function of wave number k with band index l $(= -L \leq l \leq L)$. The band index is given in increasing order of the quantity $\langle n\rangle$, where

$$\langle n\rangle = \frac{\int_{I(k)} \bar{n}(k)dk}{\int_{I(k)} dk}, \qquad \bar{n}(k) = \sum_{n=-L}^{L} n|\chi_{ln}(k)|^2, \tag{7}$$

and $\chi_{ln}(k)$ is the nth element of the eigenvector $\vec{\chi}_l(k)$. (The quantity $\langle n\rangle\hbar$ can be regarded as a mean momentum of the corresponding quasienergy band.) In Fig. 2(a) we show 22 bands with $-11 \leq l \leq 10$ for a fixed set of the parameters $(\hbar,\omega,\beta) = (0.2,0.2,0)$.

The three numerical factors (finite precision, finite truncation of $\mathbf{F}^{(k)}$, and calculation at discrete values of k) make it impossible to resolve avoided crossings with tiny width. Thus the quasienergy bands numerically obtained include some spurious regular bands whose dispersion relation is similar to that of free motion given by Eq. (6)

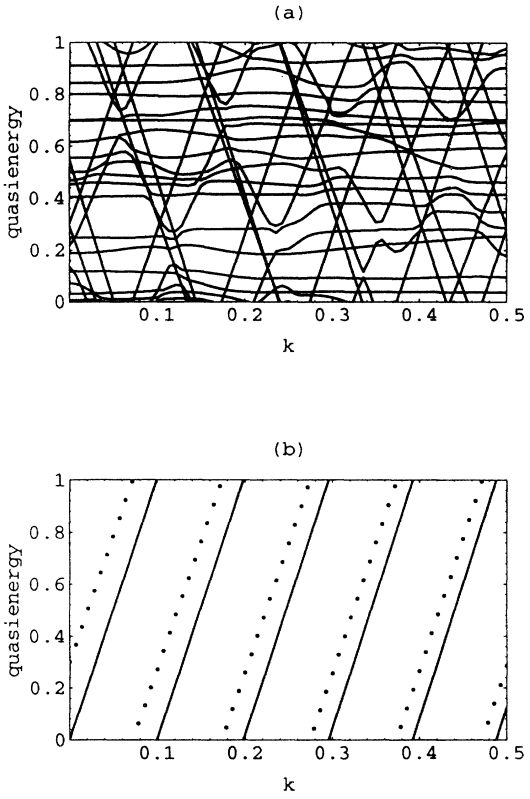

FIG. 2. (a) 22 quasienergy bands ($-11 \leq l \leq 10$) in units of $\hbar\omega$ with T invariance $(\hbar, \omega, \beta) = (0.2, 0.2, 0)$. (b) One of the dispersion curves of free motion given by Eq. (6) mod $\hbar\omega$ with $n = 10$ and $\hbar = 0.2$ (solid line). The spurious regular band of the system (3) with band index $l = 10$ for $(\hbar, \omega, \beta) = (0.2, 0.2, 0)$ is also plotted against wave number (dots).

mod $\hbar\omega$. The spurious regular band with band index l corresponds to the regular orbit satisfying Eq. (2). One of these bands with band index $l = 10$ are plotted against wave number k in Fig. 2(b), which is to be compared with the dispersion curve of free motion given by Eq. (6) with $n = 10$ and $(\hbar, \omega) = (0.2, 0.2)$ (solid line).

III. DIABATIC TRANSFORMATION AND RECONSTRUCTION OF QUASIENERGY BANDS

Figure 3(a) depicts the 20 quasienergy bands after excluding the spurious regular bands. Two different dispersion relations make it possible to distinguish the chaotic part from the regular part. The latter reminds us of free-motion-like dispersion law; on the other hand, the former has weak dependence on wave number. The transitions between the two parts in the quasienergy bands occur at the points of avoided crossings. Thus the existence of such avoided crossings makes it impossible to categorize unambiguously the quasienergy bands into *regular bands* and *chaotic bands* over the whole range of wave number k. We can, however, find a basis in which the avoided crossing becomes a real crossing in some approximation. In this basis we can reconstruct the band structure in such a way that it consists of the transformed regular and chaotic bands. To this end we extend the diabatic transformation given by Takami [10].

In the vicinity of an avoided crossing, the Floquet matrix is represented by a 2×2 matrix $\mathbf{F}(k) = \exp[-(i\tau/\hbar)\mathbf{H}(k)]$ whose elements are functions of Bloch wave number k. Then we can transform from $\mathbf{F}(k)$ to $\mathbf{F}'(k) = \exp[-(i\tau/\hbar)\mathbf{H}'(k)]$ in which diagonal elements of a Hermitian matrix $\mathbf{H}'(k)$ cross at the avoided crossing. Aside from a phase factor $e^{i\phi}$, this transformation can be uniquely defined under the following conditions for matrix elements in the transformed representation: (i) diagonal elements $\epsilon_l'(k)$ and $\epsilon_n'(k)$ of $\mathbf{H}'(k)$ cross at $k = k_0$ where the difference between the upper and lower quasienergies has the smallest value $\Delta = \epsilon_l(k) - \epsilon_n(k) > 0$, and (ii) off-diagonal elements are constant and equal to $(\Delta/2)e^{i\beta}$ and $(\Delta/2)e^{-i\beta}$, where we make the parameter β breaking T invariance coincide with β in Eq. (1). The explicit form of this transformation is $\mathbf{H}'(k) = \mathbf{P}(k)\mathbf{H}(k)\mathbf{P}(k)^{-1}$, or equivalently, $\mathbf{F}'(k) = \mathbf{P}(k)\mathbf{F}(k)\mathbf{P}(k)^{-1}$, where

$$\mathbf{H}'(k) = \begin{pmatrix} \epsilon_l'(k) & (\Delta/2)e^{i\beta} \\ (\Delta/2)e^{-i\beta} & \epsilon_n'(k) \end{pmatrix}, \tag{8a}$$

$$\mathbf{H}(k) = \begin{pmatrix} \epsilon_l(k) & 0 \\ 0 & \epsilon_n(k) \end{pmatrix},$$

$$\mathbf{P}(k) = \begin{pmatrix} Ae^{i\phi} & -Be^{-i(\phi-\beta)} \\ Be^{i(\phi-\beta)} & Ae^{-i\phi} \end{pmatrix}, \tag{8b}$$

$$A = \sqrt{\frac{1+S(k)}{2}},$$

$$B = \sqrt{\frac{1-S(k)}{2}},$$

$$S(k) = \mathrm{sgn}(k-k_0)\sqrt{1-\left[\frac{\Delta}{\epsilon_l(k)-\epsilon_n(k)}\right]^2}. \tag{8c}$$

The new basis vectors $\vec{\chi}_l'(k)$ and $\vec{\chi}_n'(k)$ are represented by a linear combination of the original quasienergy eigenvectors $\vec{\chi}_l(k)$ and $\vec{\chi}_n(k)$,

$$\begin{aligned} \vec{\chi}_l'(k) &= e^{-i\phi}[A\vec{\chi}_l(k) + Be^{i\beta}\vec{\chi}_n(k)], \\ \vec{\chi}_n'(k) &= e^{i\phi}[-Be^{i\beta}\vec{\chi}_l(k) + A\vec{\chi}_n(k)]. \end{aligned} \tag{9}$$

The new quasienergies and the squared absolute value of each elements of the new basis vectors are connected to the original ones as

$$\begin{pmatrix} \epsilon_l'(k) \\ \epsilon_n'(k) \end{pmatrix} = \begin{pmatrix} A^2 & B^2 \\ B^2 & A^2 \end{pmatrix} \begin{pmatrix} \epsilon_l(k) \\ \epsilon_n(k) \end{pmatrix},$$

$$\begin{pmatrix} |\chi_{li}'(k)|^2 \\ |\chi_{ni}'(k)|^2 \end{pmatrix} = \begin{pmatrix} A^2 & B^2 \\ B^2 & A^2 \end{pmatrix} \begin{pmatrix} |\chi_{li}(k)|^2 \\ |\chi_{ni}(k)|^2 \end{pmatrix}. \tag{10}$$

As far as the transformation between the quasienergies or the amplitude of the basis vectors is concerned, the

phase ϕ has no influence, and therefore it can be set to zero. Similarily, the parameter β breaking T invariance shows itself in the relation between the old and new basis vectors only.

When we apply the diabatic transformation, we have to know the values of k_0 and Δ. In order to obtain these as precisely as possible, we interpolate the quasienergies between two neighboring points $k = k_i$ and $k = k_{i+1}$ at which the quasienergies are numerically obtained as shown in Fig. 3(b). We use the interpolation formula of Everett [9].

The solid lines of Fig. 3(b) show the k dependence of quasienergies near an avoided crossing, and Figs. 4(a)–4(f) show the squared absolute value of the eigenvectors' elements $|\chi_{li}(k)|^2$ and $|\chi_{ni}(k)|^2$ versus the component index i $(= -L \leq i \leq L, L = 19)$ for three different values of k. Corresponding quasienergies are indicated by arrows in Fig. 3(b). We can see that the characteristics of eigenvectors alternate between the two bands, when the wave number k goes through an avoided crossing. At an avoided crossing, the difference between the two eigenvectors is not clear. The dotted lines of Fig. 3(b) are the new quasienergies $\epsilon'_l(k)$ and $\epsilon'_n(k)$ and Figs. 4(g) and 4(h) show $|\chi'_{li}(k)|^2$ and $|\chi'_{ni}(k)|^2$ calculated using a linear combination of $|\chi_{li}(k)|^2$ and $|\chi_{ni}(k)|^2$ shown in Figs. 4(c) and (d). Corresponding quasienergies are indicated in Fig. 3(b). We can see clearly the same difference between the new basis vectors as that between the original ones lying away from the avoided crossing. The basis vectors' elements shown in Fig. 4(h), like Figs. 4(b) and 4(f), distribute between $i \simeq -p_c/\hbar$ and $i \simeq p_c/\hbar$, corresponding to the chaotic region shown in Fig. 1. On the other hand, those shown in Fig. 4(g), like Figs. 4(a) and 4(e), distribute mainly in the narrower range around a nonzero component i, corresponding to a regular orbit shown in Fig. 1. (In the deeper semiclassical region, the difference is expected to be clearer.) These characteristics of the basis vectors are approximately invariant along the *diabatic* quasienergy bands.

By applying the diabatic transformation to some avoided crossings and by replacing the original quasienergies by the new ones, we can combine some regular parts of different bands into one diabatic regular band. We can construct these systematically one by one as follows. After excluding the spurious regular bands, the bands with the largest $|\langle n \rangle|$ have the largest regular part. We find a partner band which succeeds to the regular part across an avoided crossing. If two or more partner bands exist,

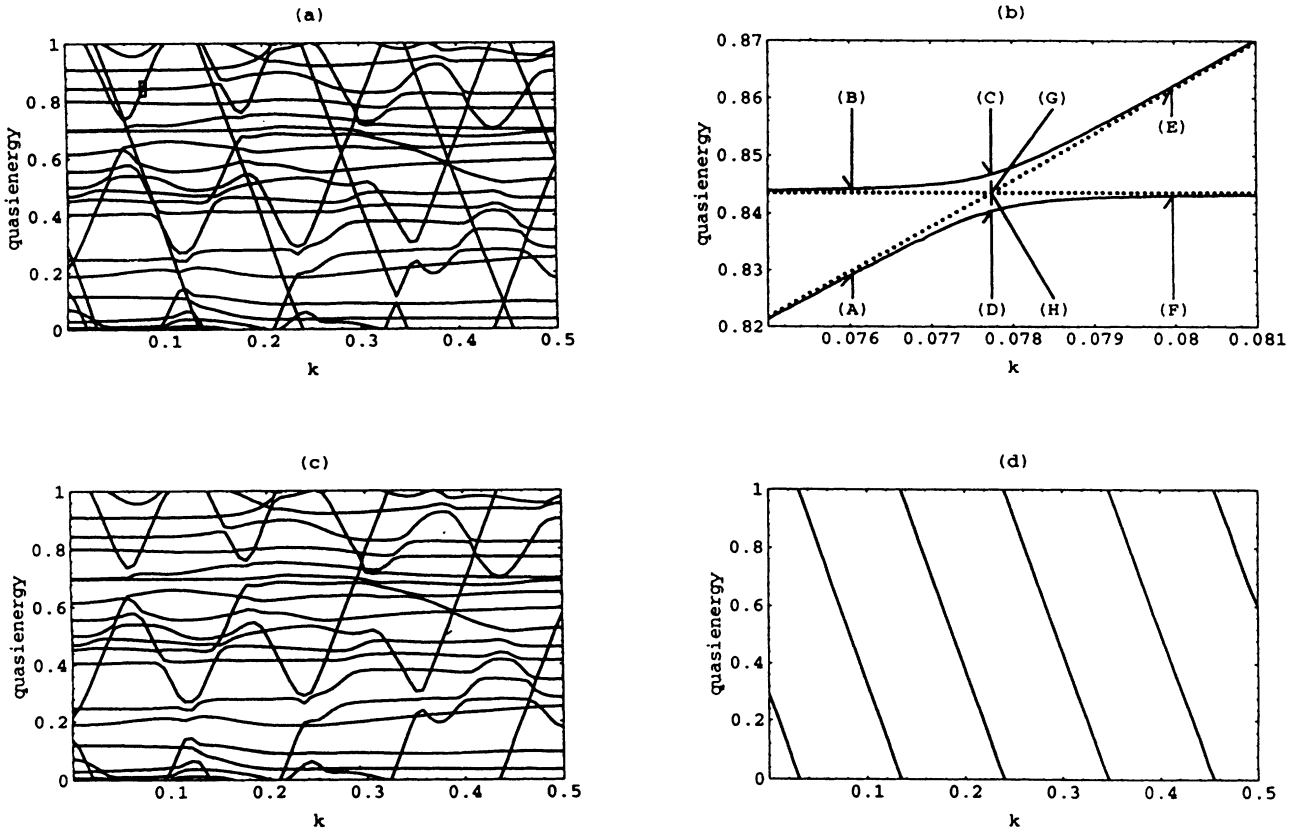

FIG. 3. Quasienergy bands in units of $\hbar\omega$ with T invariance $(\hbar, \omega, \beta) = (0.2, 0.2, 0)$. (a) 20 quasienergy bands $\epsilon_l(k)$ after excluding spurious regular bands. (b) Quasienergies (solid lines) and transformed quasienergies (dashed line) given by Eq. (10) in the vicinity of an avoided crossing. The region is enclosed by the small rectangle in (a). (c) 19 bands after excluding one diabatic regular band shown in (d). (d) One diabatic regular band removed from the bands shown in (a). Note that the quasienergies shown in (c) and (d) are partially transformed by the diabatic transformation.

we choose the band that has the least value of Δ. Then we apply the diabatic transformation to the two bands over the interval in which the distance $|\epsilon_l(k) - \epsilon_n(k)|$ grows monotonically as a function of $|k - k_0|$. After that we renumber the band indices of the whole bands. By repeating the above scheme, we can construct a regular band whose dispersion relation is similar to that of free motion given by Eq. (6) mod $\hbar\omega$ over the whole range of k. Fig. 3(d) depicts such a band constructed from the original bands shown in Fig. 3(a), and the rest of the bands are shown in Fig. 3(c). So far we removed the regular bands corresponding to the regular trajectories satisfying Eq. (2) with $|l| \geq 10$.

We can observe in Fig. 3(b) the next candidate of regular bands to be removed. Corresponding avoided crossings are partially narrow, but partially wide. The wider the avoided crossing, the harder the transformation. We quit the procedure of creating a regular band, unless all the widths of the avoided crossings concerned are less than the mean spacing given by [$\hbar\omega$/(the number of the surviving bands)]. Thus we cannot exclude the next regular band from the bands shown in Fig. 3(b), which remains intact as a broken regular band. We can find one more broken regular band with a negative slope by a careful observation. The two broken regular bands correspond to the regular trajectories satisfying Eq. (2) with $|l| = 9$.

In this sense a complete exclusion of regular bands is

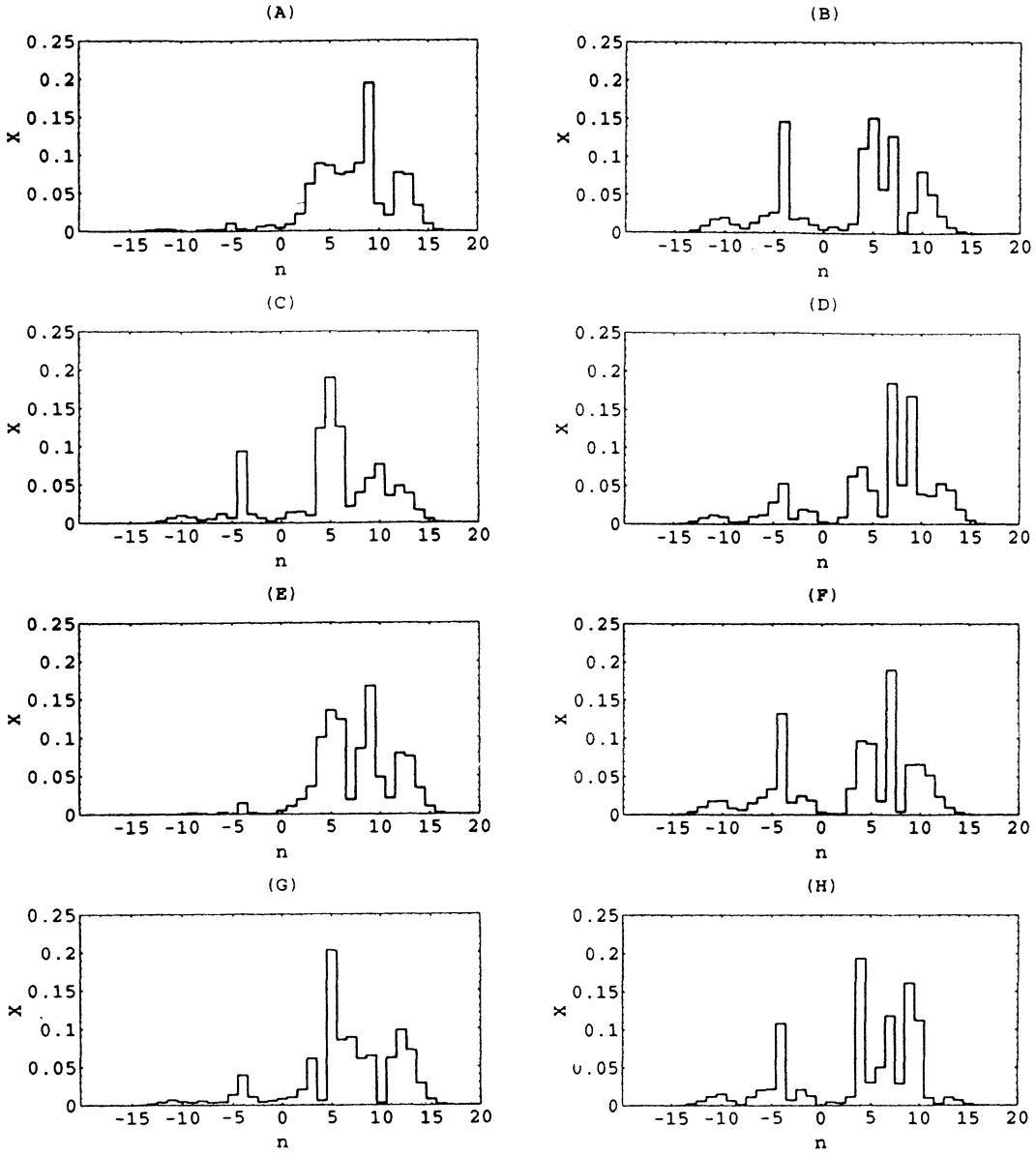

FIG. 4. (a)-(f) Squared absolute value X of elements of quasienergy eigenvectors. (g) and (h) That of the transformed basis vectors calculated from the eigenvectors displayed in (c) and (d). Corresponding quasienergies are indicated in Fig. 3(b).

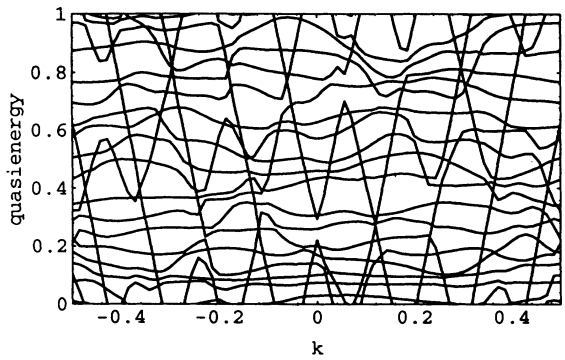

FIG. 5. Quasienergy bands in units of $\hbar\omega$ without T invariance $(\hbar, \omega, \beta) = (0.2, 0.2, 1)$ after excluding all spurious regular bands.

impossible even with the diabatic transformation. This difficulty comes from the absence of a definite "boundary" between the chaotic and the regular bands in contrast to the Poincaré section shown in Fig. 1. Nevertheless, the method of excluding regular bands suggested here is believed to be the best way as a well-defined procedure. As we mentioned before, the minimum width of the avoided crossing that can be resolved in our method depends on the precision or other numerical factors. The smaller avoided crossings are resolved with a higher degree of accuracy, the more diabatic transformations are required. But the final band structure is independent of a minute difference of precision, if the precision is good enough.

The case without T invariance $(\hbar, \omega, \beta) = (0.2, 0.2, 1)$ is also considered. The Poincaré section seems almost the same as Fig. 1. The final band structure after the exclusion of the regular bands is shown in Fig. 5.

IV. NEAREST-NEIGHBOR-SPACING STATISTICS OF QUASIENERGY BANDS

The final band structure shown in Fig. 3(c) and Fig. 5 contains two broken regular bands, so that the distribution of band spacings $P(s)$ is expected to be intermediate between Poisson and Wigner. One of the interpolations is given by the Brody distribution [11] $P_B(s, q)$ for the case with T invariance and its extension $\tilde{P}_B(s, q)$ for the case without one, where

$$P_B(s, q) = A_q s^q \exp[-B_q s^{1+q}], \tag{11a}$$

$$\tilde{P}_B(s, q) = \tilde{A}_q s^{2q} \exp[-\tilde{B}_q s^{1+q}]. \tag{11b}$$

The constants $A_q, B_q, \tilde{A}_q$, and $\tilde{B}_q$ are determined by the normalization $\langle 1 \rangle = 1$ and the mean spacing $\langle s \rangle = 1$, and these are dependent on the fitting parameter q. We show the integrated distribution of band spacings $I(s) = \int_0^s P(t)dt$ in Fig. 6(a) for the case with T invariance and (b) without one, in addition to the best fit

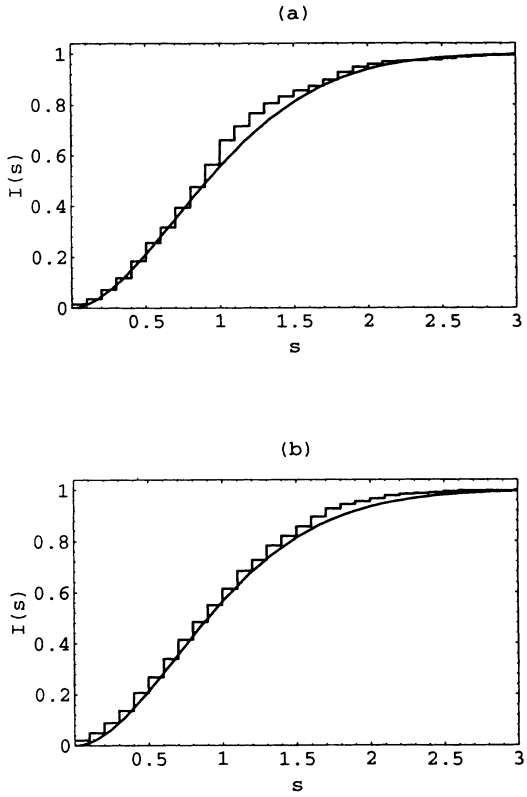

FIG. 6. Integrated distribution functions $I(S)$ of the band spacing S, which is normalized by the value of $\hbar\omega$ divided by the number of the surviving bands. The best fit of the distribution Eq. (11) is also shown. (a) $(\hbar, \omega, \beta) = (0.2, 0.2, 0)$ with T invariance. (b) (0.2,0.2,1) without one. The histograms (a) and (b) correspond to Fig. 3(c) and Fig. 5, respectively.

of Eq. (11). The fitting parameter is given by $q = 0.776$ for Fig. 6(a) and $q = 0.487$ for 6(b). At the stage corresponding to Fig. 3(a), the spacing distribution is fitted by the Brody distribution with $q = 0.687$ for the case with T invariance and $q = 0.428$ for the case without one. Apparently the distribution approaches the Wigner surmise, as the procedure excluding the regular bands goes ahead. The deviation from the Wigner distribution $(q = 1)$ is expected to be caused by the existence of the broken regular bands.

V. CONCLUDING REMARKS

We have proposed a transformation which allows us to separate quasienergy bands of the model into bands associated only with the classical regular trajectories and bands associated only with the chaotic trajectories. This is not always trivial, since the original band may be partially regular and partially chaotic. The separation of the spectrum is then used to obtain level spacing statistics of the transformed bands associated with the classical chaotic trajectories. The nearest-neighbor-spacing distribution is found to be in a good agreement with the Brody distribution.

We note that, besides the Brody distribution, the Berry-Robnik distribution [12] might be relevant to the problem of interest. The latter has the form

$$P_2(s,\rho) = \rho^2 e^{-\rho s}\mathrm{erfc}\left[\frac{\sqrt{\pi}}{2}\bar{\rho}s\right] + \left(2\rho\bar{\rho} + \frac{\pi}{2}\rho^3 s\right) \times \exp\left[-\rho s - \frac{\pi}{4}\bar{\rho}^2 s^2\right], \quad (12a)$$

and its extension for the case without T invariance is given by

$$\tilde{P}_2(s,\rho) = \rho\bar{\rho}(2-\rho s)e^{-\rho s}\mathrm{erfc}\left[\frac{2}{\sqrt{\pi}}\bar{\rho}s\right] + \left(\rho^2 + \frac{8}{\pi}\bar{\rho}^2\rho s + \frac{32}{\pi^2}\bar{\rho}^4 s^2\right) \times \exp\left[-\rho s - \frac{4}{\pi}\bar{\rho}^2 s^2\right]. \quad (12b)$$

These are derived from the assumption that a sequence of regular levels and that of chaotic levels are statistically independent of each other, and the parameter $\rho = 1-\bar{\rho}$ is the relative volume of regular region in the phase space. A remarkable character of these distributions is a nonvanishing density at 0 spacing $P_2(0,\rho) = \tilde{P}_2(0,\rho) = \rho(2-\rho)$ in contrast to $P_B(0,q) = \tilde{P}_B(0,q) = 0$. In our case almost all the crossing between the regular and the chaotic bands is avoided, so that the mixed sequence of levels should obey a Brody-type distrubution. However, after the reconstructing process which separates the bands into regular and chaotic ones, the nearest-neighbor-spacing distribution of the mixture of the regular and chaotic diabatic bands is expected to be the Berry-Robnik type. The separation of quasienergy bands justifies the assumption of statistical independence. This can be confirmed with much more time- and space-consuming numerical works in a deeper semiclassical limit. Quite recently, Prosen and Robnik showed numerically that a transition from the Brody to Berry-Robnik distribution occurs as a very deep semiclassical limit is taken, and that the assumption of statistical independence required in the Berry-Robnik theory is satisfied in this limit [13]. We note that the separation of the spectrum discussed in the present paper satisfies automatically the assumption even in a less semiclassical limit.

We would also like to note one advantage of our model. Because of translational symmetry, we can always consider the ensemble of wave-number-dependent Hamiltonians like $\hat{H}^{(k)}$ in (3d) corresponding to a classical Hamiltonian H in (1) at a fixed value of external parameter. Conventionally (without translational symmetry) some sets of samples for different values of the parameter (e.g., ω in our case) are used for statistics. But the classical quantity like the Lyapunov exponent or the relative regular volume ρ varies usually during the variation of parameter. We note that the case with translational symmetry enables us to get statistics by considering wave-number-dependent Hamiltonian or Floquet matrices for different values of wave number but for a fixed value of external parameter, as considered in the present paper.

In the end we note that the problem considered here is related to the problem of the quantum counterpart of the diffusion process in the chaotic region. If it were not for the coupling between chaotic and regular states, an initial wave packet located in the chaotic region *diffusively* collapses as $\langle x^2\rangle \propto t$ in the time regime $t \ll t_c$, where a characteristic time t_c is given by the inverse of the mean band spacing of the final band structure [e.g., Fig. 3(c) or Fig. 5] times Planck's constant. But the existence of the coupling gives an appreciable contribution of *ballistic* widening of the wave packet as $\langle x^2\rangle \propto t^2$. Thus it is very useful to obtain the final band structure by use of our method in order to discuss the quantal counterpart of diffusion in the coordinate space. The detail of dynamical aspects and an experimental realization are described in Ref. [5]. In this sense the present paper and Ref. [5] are complementary to each other.

ACKNOWLEDGMENTS

This work is supported by the Deutsche Forschungsgemeinschaft through its Sonderforschungsbereich 237. S.M. and A.R.K acknowledge financial support through, respectively, the Deutscher Akademischer Austauschdienst (DAAD) and the Alexander von Humboldt-Stiftung. We thank Robert Graham, Fritz Haake, András Csordás, and Karol Życzkowski for stimulating discussions and for a careful reading of the manuscript. We also thank Marko Robnik for providing us his unpublished paper [13].

[1] O. Bohigas and M.-J. Giannoni, in *Mathematical and Computational Methods in Nuclear Physics*, Proceedings of the Sixth Granada Workshop, Granada, Spain, 1983, edited by J. S. Dehesa, J. M. G. Gomez, and A. Polls, Lecture Notes in Physics Vol. 209 (Springer, Berlin, 1984).
[2] F.M. Izrailev, Phys. Rep. **196**, 299 (1990).
[3] F. Haake, *Quantum Signature of Chaos* (Springer, Berlin, 1992).
[4] R. Graham and J. Keymer, Phys. Rev. A **44**, 6281 (1991).
[5] A.R. Kolovsky, S. Miyazaki, and R. Graham, Phys. Rev. E **49**, 70 (1994).
[6] T. Geisel, A. Zacherl, and G. Radons, Z. Phys. B **71**, 117 (1988); D. Weiss, M.L. Roukes, A. Menschig, P. Grambow, K.v. Klitzig, and G. Weimann, Phys. Rev. Lett. **66**, 2790 (1991); R. Fleischmann, T. Geisel, and R. Ketzmerick, *ibid.* **68**, 1367 (1992).
[7] J.D. Lambert, *Numerical Methods for Ordinary Differential Systems* (Wiley, Chichester, 1991).
[8] J.S. Howland, Ann. Inst. Henri Poincaré, Phys. Theor. **50**, 309 (1989); **50**, 325 (1989).
[9] *Handbook of Mathematical Functions*, edited by M. Abramowitz and I.A. Stegun (Dover, New York, 1970).
[10] T. Takami, Phys. Rev. Lett. **68**, 3371 (1992).
[11] T.A. Brody, Lett. Nuovo Cimento **12**, 482 (1973).
[12] M.V. Berry and M. Robnik, J. Phys. A **17**, 2413 (1984).
[13] T. Prosen and M. Robnik (unpublished).